Received: 26 October 2021 | Revised: 21 January 2022 | Accepted: 7 February 2022

IET Signal Processing

DOI: 10.1049/sil2.12110

The Institution of Engineering and Technology WILEY

ORIGINAL RESEARCH

Joint waveform and precoding design for coexistence of MIMO radar and MU-MISO communication

Tong Wei | **Linlong Wu** | **Bhavani Shankar Mysore Rama Rao**

Interdisciplinary Centre for Security, Reliability and Trust (SnT), University of Luxembourg, Luxembourg

Correspondence

Linlong Wu, Interdisciplinary Centre for Security, Reliability and Trust (SnT), University of Luxembourg , Luxembourg, L-1855, Luxembourg.
Email: linlong.wu@uni.lu

Funding information

CORE project "SPRINGER", Luxembourg National Research Fund (FNR), Grant/Award Number: ref 12734677

[Corrections added on 02-May-2022, after first online publication: The legal statement was replaced with the following: This is an open access article under the terms of the Creative Commons Attribution License, which permits use, distribution and reproduction in any medium, provided the original work is properly cited.]

Abstract

The joint design problem for the coexistence of multiple-input multiple-output (MIMO) radar and multi-user multiple-input-single-output (MU-MISO) communication is investigated. Different from the conventional design schemes, which require defining the primary function, we consider designing the transmit waveform, precoding matrix and receive filter to maximize the radar SINR and the minimal SINR of communication users, simultaneously. By doing so, the promising overall performance for both sensing and communication is achieved without requiring parameter tuning for the threshold of communication or radar. However, the resulting optimization problem which contains the maximin objective function and the unit sphere constraint, is highly nonconvex and hence difficult to attain the optimal solution directly. Towards this end, the epigraph-form reformulation is first adopted, and then an alternating maximisation (AM) method is devised, in which the Dinkelbach's algorithm is used to tackle the nonconvex fractional-programing subproblem. Simulation results indicate that the proposed method can achieve improved performance compared with the benchmarks.

KEYWORDS

MIMO communication, MIMO radar, precoding, radar signal processing

1 | INTRODUCTION

With the rapid growth of wireless applications, spectrum congestion has become a severe problem which limits the efficiency of data transmission. To tackle this issue, the next-generation communication networks are required to share the frequency band with other radio-frequency (RF) systems [1, 2]. As a representative configuration, the joint radar-communication (JRC) has attracted great attention in recent years [3–10], which shares the frequency and other resources between radar and communication. Based on whether both radar and communication share the same transmit platform, most of the current JRC systems can be roughly classified into two categories, that is, dual-function radar-communication (DFRC) [11–19] and coexistence of radar and communication [20–29].

With regards to the DFRC, the dual-function base-station (DFBS) emits a set of waveform to illuminate the target and communicate to the users simultaneously [11–18, 30–33]. Meanwhile, the corresponding radar and communication receivers can process the received signal and hence further extract the related system parameters [13, 16]. Leveraging on the advantage of platform sharing, the DFRC system is able to reduce hardware cost and enhance energy efficiency. For example, in Ref. [11], the transmit waveform is considered to shape a desired radar beampattern while ensuring a required communication rate. Considering the consumption of hardware resources, in Ref. [13], the sparse array configuration which requires fewer radio frequency (RF) chains is developed for DFRC. Moreover, in Ref. [14], the low-resolution DACs are deployed at the DFBS to further reduce the hardware complexity. Meanwhile, the authors minimise the mean-squared error (MSE) of symbol recovery while keeping a preferable target localization performance in Ref. [14]. Then, in Ref. [15], the hybrid beamforming architecture is utilised in the wideband DFRC system and the beampattern and achievable

sum-rate are considered as the metrics for radar and communication, respectively. Recently, the automotive DFRC system is developed in Ref. [18] in which the method can provide a flexible trade-off between the radar and communication performances. Moreover, the wideband DFRC which emits the orthogonal frequency division multiplexing (OFDM) waveform is considered in Ref. [31]. With a properly designed subcarrier selection and power allocation scheme, the total transmit power from the DFRC system is minimised while both the mutual information and the communication rate are guaranteed to meet the requirement.

For the coexistence scheme, radar and communication systems operate independently with their own set of separate waveforms [5, 20–29]. Compared with DFRC, the coexistence structure shows the flexibility in transmitter deployment and waveform design. However, the mutual interference (MI) between radar and communication systems is inevitable in this scenario. Thus, many works generally focus on eliminating the MI. For example, in Ref. [5], the matrix completion (MC)-based multiple-input multiple-output (MIMO) radar shares the spectrum with MIMO communication. The covariance matrix of communication symbol is synthesised to reduce the effective interference power (EIP) at the radar receiver which is regarded as the radar-centric method. Considering the practical constraints for radar signal, in Ref. [20], the total transmit power from the JRC system is minimised while ensuring that the radar SINR and the symbol detection MSE are better than a predefined threshold. Furthermore, in Ref. [21], the radar waveform, the receive filter and the communication symbol covariance are jointly designed to maximize the radar SINR under the communication sum-rate constraint. In order to simplify the implementation, in Ref. [23], the discrete-phase sequence is utilised in the coexistence system. Different from the aforementioned schemes, in Ref. [25], the achievable communication sum-rate is maximised under the radar SINR constraint which is considered as the communication-centric method. In Ref. [29], the coexistence scheme is extended to the wideband case. Leveraging on the OFDM transmission, three different radar waveform design criteria are developed to minimise the worst-case transmit power of the radar system with the minimum capacity constraint for the communication system.

It is worth pointing out that the above-mentioned coexistence schemes optimise the radar performance metrics under the communication constraints (i.e., radar-centric) or vice versa (i.e., communication-centric). From this perspective, the objective function is either radar-only or communication-only. Hence, the above method cannot achieve a preferable performance for radar and communication, simultaneously. Motivated by the limitation, we focus on designing the transmit waveform, receive filter and precoding matrix for coexistence of the MIMO radar and multi-user multiple-input-single-output (MU-MISO) communication system. The corresponding problem is to maximize both the radar SINR and the minimal SINR among all communication users simultaneously under some practical waveform constraints. The main contributions of this paper are summarised as follows:

- A novel optimization problem is formulated for the coexistence of MIMO radar and MU-MISO communication, which aims to maximize the radar SINR and the minimal SINR among multiple users simultaneously. Therefore, it can improve the performance for both radar and communication systems.
- The resulting optimization problem is nonconvex, in which the objective function consists of two quadratic fractional terms. To tackle this problem, an alternating maximisation (AM) method is proposed. Moreover, the difference of convex programing (DCP) [34] and the Dinkelbach method [35] are, respectively, introduced to deal with the related subproblems.
- Numerical results are provided to illustrate the excellent performance of the proposed algorithm in terms of the receiver beampattern, ambiguity function, SINR of the radar system and the minimal communication SINR. As expected, in our proposed method, both the radar SINR and the minimal SINR of users are enhanced expressing the superiority of the proposed method compared to the benchmark.

The remainder of this paper is organised as follows. The signal model and problem formulation for coexistence of MIMO radar and MU-MISO communication are firstly introduced in Section 2. Next, Section 3 introduces a novel AM-based algorithm which is used to tackle the aforementioned nonconvex problem. In Section 4, we utilise various numerical examples to demonstrate the effectiveness of the proposed method. Finally, Section 5 summarises this work.

Notation: Vectors and matrices are denoted by lower case boldface letters and upper case boldface letters, respectively. $(\cdot)^T$, $(\cdot)^*$ and $(\cdot)^H$ denote the operations of transpose, conjugate, and Hermitian transpose, respectively. $\mathbf{I}_L$ denotes the $L \times L$ identity matrix and $\otimes$ is the Kroneker product. $\Re(\cdot)$ and $\Im(\cdot)$ denote the real part and imaginary part of a complex number, respectively. The operator vec$(\cdot)$ denotes the vectorisation of a matrix. Finally, $\|\cdot\|_2$ and $\|\cdot\|_F$ represent the ℓ_2-norm and Frobenius-norm, respectively.

2 | SYSTEM MODEL AND PROBLEM FORMULATION

As illustrated in Figure 1, a MU-MISO communication system coexists with a narrow-band colocated MIMO radar, both of which share the same frequency band. The MIMO radar system deploys N_t transmit and N_r receive antennas to sense the single moving target under the K stationary clutter patches. In the communication system, the base-station (BS) is equipped with M_t antennas serving M_r single-antenna users. Further, we assume that the sample time of the radar and communication systems is perfectly synchronized [5].

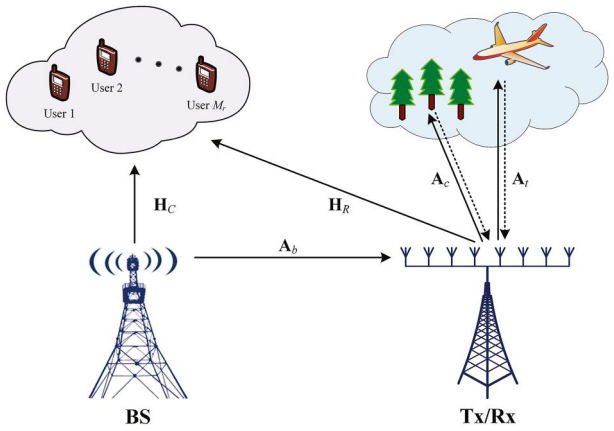

FIGURE 1 Coexistence of MIMO radar and MIMO communication

2.1 | Radar system

We denote $\mathbf{s}(l) = [s_1(l), \ldots, s_{N_t}(l)]^T$ as the transmitted signal of the radar system, where $l = 1, \ldots, L$ with L being the number of discrete time samples. Consider a far-field moving target at the angle θ_0, the received signal of the radar system at the l-th time instance can be given by [21]

$$\begin{aligned}\mathbf{y}_R(l) &= \alpha_0 e^{j2\pi v_t(l-1)}\mathbf{a}_r^*(\theta_0)\mathbf{a}_t^H(\theta_0)\mathbf{s}(l) \\ &\quad + \sum_{k=1}^{K}\alpha_k \mathbf{a}_r^*(\theta_k)\mathbf{a}_t^H(\theta_k)\mathbf{s}(l) \\ &\quad + \mathbf{A}_b\mathbf{G}\mathbf{x}(l) + \mathbf{n}_R(l) \\ &= \mathbf{A}_t\mathbf{s}(l) + \mathbf{A}_c\mathbf{s}(l) + \mathbf{A}_b\mathbf{G}\mathbf{x}(l) + \mathbf{n}_R(l),\end{aligned} \tag{1}$$

where

- α_0 is the reflection parameter of the target which is related to radar cross section (RCS) and propagation loss. Similarly, α_k, $k = 1, \ldots, K$, denote the RCS of kth clutter patch. v_t is the normalized Doppler frequency of the target.
- $\mathbf{a}_t(\theta) = \left[1, e^{j\pi\sin(\theta)}, \ldots, e^{j\pi(N_t-1)\sin(\theta)}\right]^T$ is the radar transmit steering vector.
- Similarly, $\mathbf{a}_r(\theta) = \left[1, e^{j\pi\sin(\theta)}, \ldots, e^{j\pi(N_r-1)\sin(\theta)}\right]^T$ is the receiver steering vector.
- $\mathbf{G} = \left[\mathbf{g}_1, \ldots, \mathbf{g}_{M_r}\right] \in C^{M_t\times M_r}$ denotes the precoding matrix.
- $\mathbf{x}(l) = [x_1(l), \ldots, x_{M_r}(l)]^T$ is the normalized symbol stream to communicate with M_r users at l-th time instance, $\forall l = 1, \ldots, L$. Meanwhile, it is assumed that $\mathbb{E}\{\mathbf{x}(l)\mathbf{x}^H(l)\} = \mathbf{I}_{M_r}$, that is, the normalized orthogonal transmit code words are used.
- $\mathbf{n}_R(l)$, $l = 1, \ldots, L$ is the additive noise which is also modelled as complex circular zero-mean Gaussian random vector, that is, $\mathbf{n}_R(l) \sim \mathcal{CN}\left(0, \sigma_{n,R}^2\mathbf{I}_{N_r}\right)$.
- $\mathbf{A}_t$ and $\mathbf{A}_c$ denote the response matrix for target and clutters, respectively. $\mathbf{A}_b$ denotes the channel matrix which couples the base-station (BS) and radar receiver.

We rewrite the received signal of all time instances into a compact form as follows:

$$\mathbf{Y}_R = \mathbf{A}_t\mathbf{S} + \mathbf{A}_c\mathbf{S} + \mathbf{A}_b\mathbf{G}\mathbf{X} + \mathbf{N}_R, \tag{2}$$

where $\mathbf{S} = [\mathbf{s}(1), \ldots, \mathbf{s}(L)]$, $\mathbf{X} = [\mathbf{x}(1), \ldots, \mathbf{x}(L)]$ and $\mathbf{N}_R = [\mathbf{n}_R(1), \ldots, \mathbf{n}_R(L)]$. Then, we can vectorise $\mathbf{Y}_R$ in Equation (2) as

$$\mathbf{y}_R = (\mathbf{I}_L \otimes \mathbf{A}_t)\mathbf{s} + (\mathbf{I}_L \otimes \mathbf{A}_c)\mathbf{s} + (\mathbf{I}_L \otimes \mathbf{A}_b\mathbf{G})\mathbf{x} + \mathbf{n}_R, \tag{3}$$

where $\mathbf{y}_R = \left[\mathbf{y}_R^T(1), \ldots, \mathbf{y}_R^T(L)\right]^T$, $\mathbf{s} = \left[\mathbf{s}^T(1), \ldots, \mathbf{s}^T(L)\right]^T$, $\mathbf{x} = \left[\mathbf{x}^T(1), \ldots, \mathbf{x}^T(L)\right]^T$ and $\mathbf{n}_R = \left[\mathbf{n}_R^T(1), \ldots, \mathbf{n}_R^T(L)\right]^T$.

Using the receive filter $\mathbf{w}$ to reduce the interference and noise, the output signal of the radar receiver is

$$\begin{aligned}\mathbf{w}^H\mathbf{y}_R = {} & \mathbf{w}^H(\mathbf{I}_L \otimes \mathbf{A}_t)\mathbf{s} + \mathbf{w}^H(\mathbf{I}_L \otimes \mathbf{A}_c)\mathbf{s} \\ & + \mathbf{w}^H(\mathbf{I}_L \otimes \mathbf{A}_b\mathbf{G})\mathbf{x} + \mathbf{w}^H\mathbf{n}_R,\end{aligned} \tag{4}$$

where $\mathbf{w} = \left[\mathbf{w}_1^T, \ldots, \mathbf{w}_L^T\right]^T$ and $\mathbf{w}_l$ denote the receiver filter at l-th time instant. According to Equation (4), the output radar SINR is

$$\begin{aligned}&\mathrm{SINR}_r \\ &= \frac{|\mathbf{w}^H(\mathbf{I}_L \otimes \mathbf{A}_t)\mathbf{s}|^2}{|\mathbf{w}^H(\mathbf{I}_L \otimes \mathbf{A}_c)\mathbf{s}|^2 + \mathbb{E}\{|\mathbf{w}^H(\mathbf{I}_L \otimes \mathbf{A}_b\mathbf{G})\mathbf{x}|^2\} + \mathbb{E}\{|\mathbf{w}^H\mathbf{n}_R|^2\}} \\ &= \frac{|\mathbf{w}^H(\mathbf{I}_L \otimes \mathbf{A}_t)\mathbf{s}|^2}{|\mathbf{w}^H(\mathbf{I}_L \otimes \mathbf{A}_c)\mathbf{s}|^2 + \|\mathbf{w}^H(\mathbf{I}_L \otimes \mathbf{A}_b\mathbf{G})\|_2^2 + \sigma_{n,R}^2\mathbf{w}^H\mathbf{w}}.\end{aligned} \tag{5}$$

where $E[\mathbf{x}\mathbf{x}^H] = \mathbf{I}$ is used.

2.2 | Communication system

For all users, the received data at the l-th time instance is written as

$$\mathbf{y}_C(l) = \mathbf{H}_C\mathbf{G}\mathbf{x}(l) + \mathbf{H}_R\mathbf{s}(l) + \mathbf{n}_C(l) \in \mathbb{C}^{M_r\times 1}, \tag{6}$$

where $\mathbf{H}_C \in \mathbb{C}^{M_r\times M_t}$ denotes the downlink channel coupling BS and the users, $\mathbf{H}_R \in \mathbb{C}^{M_r\times N_t}$ is the interference channel coupling the radar transmitter and the users and $\mathbf{n}_C(l) \sim \mathcal{CN}\left(0, \sigma_{n,C}^2\mathbf{I}_{M_r}\right)$ denotes the noise vector of the communication system. Collecting the received signals for all time instances in a compact form, we have

$$\mathbf{Y}_C = \mathbf{H}_C\mathbf{G}\mathbf{X} + \mathbf{H}_R\mathbf{S} + \mathbf{N}_C. \tag{7}$$

Hence, for m_r-th user, the received data stream is

$$\mathbf{y}_{m_r,C} = \mathbf{h}_{m_r,C}\mathbf{G}\mathbf{X} + \mathbf{h}_{m_r,R}\mathbf{S} + \mathbf{n}_{m_r,C} \tag{8}$$

where $\mathbf{y}_{m_r,C}$, $\mathbf{h}_{m_r,C}$, $\mathbf{h}_{m_r,R}$ and $\mathbf{n}_{m_r,C}$ denote the m_r-th row of $\mathbf{Y}_C$, $\mathbf{H}_C$, $\mathbf{H}_R$ and $\mathbf{N}_C$, respectively. According to Equation (8), the output SINR for m_r-th user is readily given by

$$\begin{aligned}&\mathrm{SINR}_c^{m_r}\\ =\ &\frac{\mathbb{E}\left\{\|\mathbf{h}_{m_r,C}\mathbf{G}\mathbf{\Lambda}_{m_r}\mathbf{X}\|_2^2\right\}}{\mathbb{E}\left\{\sum\limits_{i\neq m_r}\|\mathbf{h}_{m_r,C}\mathbf{G}\mathbf{\Lambda}_i\mathbf{X}\|_2^2+\|\mathbf{h}_{m_r,R}\mathbf{S}\|_2^2+\|\mathbf{n}_{m_r,C}\|_2^2\right\}}\\ =\ &\frac{|\mathbf{h}_{m_r,C}\mathbf{g}_{m_r}|^2}{\sum\limits_{i\neq m_r}|\mathbf{h}_{m_r,C}\mathbf{g}_i|^2+\frac{1}{L}\|(\mathbf{I}_L\otimes\mathbf{h}_{m_r,R})\mathbf{s}\|_2^2+\sigma_{n,C}^2},\end{aligned}\tag{9}$$

where $\mathbf{\Lambda}_{m_r}$ is the diagonal matrix whose m_r-th diagonal entry is one and others are zero. For the communication system, two typical metrics, that is, *throughput* and *fairness* [24], are usually considered to measure the communication system performance. The throughput aims to maximize the overall sum-rate while the fairness focuses on improving the minimal SINR among all users [36]. The fairness design is considered.

2.3 | Problem formulation

For the radar system, the performance of target detection can be enhanced via maximising the output SINR. With regard to the communication system, we aim to achieve the fairness among all users. Based on the above illustration, the joint design problem is formulated as

$$\begin{aligned}\max_{\mathbf{w},\mathbf{s},\mathbf{G}}\quad &\mathrm{SINR}_r+\min_{m_r}\left\{\mathrm{SINR}_c^{m_r}\right\}\\ s.t.\quad &\|\mathbf{s}\|_2^2=1,\\ &\|\mathbf{G}\|_F^2\le P_c,\\ &\|\mathbf{s}-\mathbf{s}_0\|_2^2\le\xi,\end{aligned}\tag{10}$$

where P_c denotes the maximum transmit power of the communication system, $\|\mathbf{s}\|^2=1$ represents the normalized transmit power of the radar system, and $\|\mathbf{s}-\mathbf{s}_0\|^2\le\xi$ is the similarity constraint with $0\le\xi<2^2$.

Problem (Equation 10) involves a maximin objective function and a nonconvex unit sphere constraint and thereby is NP-hard [25, 37]. To tackle this problem, we introduce an auxiliary variable t and equivalently reformulate the problem (Equation 10) into its epigraph form as follows:

$$\begin{aligned}\max_{t,\mathbf{w},\mathbf{s},\mathbf{G}}\quad &\mathrm{SINR}_r+t\\ s.t.\quad &\mathrm{SINR}_c^{m_r}\ge t,m_r=1,\ldots,M_r,\\ &\|\mathbf{s}\|_2^2=1,\\ &\|\mathbf{G}\|_F^2\le P_c,\\ &\|\mathbf{s}-\mathbf{s}_0\|_2^2\le\xi.\end{aligned}\tag{11}$$

Then, an alternating maximisation (AM)-based approach will be devised to tackle the problem (Equation 11).

3 | JOINT DESIGN VIA ALTERNATING MAXIMIZATION

Instead of solving the problem (Equation 11) directly, following the updated rules of the alternating maximisation (AM) algorithm, we update four variables via solving the subproblems with respect to t, $\mathbf{w}$, $\mathbf{s}$ and $\mathbf{G}$, iteratively, until convergence is reached. We will discuss the detailed updated procedures in the sequel.

3.1 | Update the receive filter w

With the given $\mathbf{s}$ and $\mathbf{G}$, the optimization problem with respect to the radar receiver filter $\mathbf{w}$ can be expressed as

$$\max_{\mathbf{w}}\quad\frac{|\mathbf{w}^H(\mathbf{I}_L\otimes\mathbf{A}_t)\mathbf{s}|^2}{|\mathbf{w}^H(\mathbf{I}_L\otimes\mathbf{A}_c)\mathbf{s}|^2+\|\mathbf{w}^H(\mathbf{I}_L\otimes\mathbf{A}_b\mathbf{G})\|^2+\sigma_{n,R}^2\|\mathbf{w}\|_2^2}.\tag{12}$$

Noted that the problem (Equation 12) is the conventional SINR maximisation problem which is equivalent to the minimum variance distortionless response (MVDR) problem [23, 38]. Hence, the close-form solution of Equation (12) is immediately given by

$$\mathbf{w}=\frac{(\mathbf{R}(\mathbf{s},\mathbf{G}))^{-1}(\mathbf{I}_L\otimes\mathbf{A}_t)\mathbf{s}}{\mathbf{s}^H(\mathbf{I}_L\otimes\mathbf{A}_t^H)(\mathbf{R}(\mathbf{s},\mathbf{G}))^{-1}(\mathbf{I}_L\otimes\mathbf{A}_t)\mathbf{s}},\tag{13}$$

where

$$\begin{aligned}\mathbf{R}(\mathbf{s},\mathbf{G})=\ &\sigma_{n,R}^2\mathbf{I}_{NL}+(\mathbf{I}_L\otimes\mathbf{A}_c)\mathbf{s}\mathbf{s}^H(\mathbf{I}_L\otimes\mathbf{A}_c^H)\\ &+(\mathbf{I}_L\otimes\mathbf{A}_b\mathbf{G})(\mathbf{I}_L\otimes\mathbf{G}^H\mathbf{A}_b^H).\end{aligned}\tag{14}$$

3.2 | Update the precoding matrix G

For the fixed t, $\mathbf{w}$ and $\mathbf{s}$, the problem with respect to $\mathbf{G}$ is

$$\begin{aligned}\max_{\mathbf{G}}\quad &\frac{|\mathbf{w}^H(\mathbf{I}_L\otimes\mathbf{A}_t)\mathbf{s}|^2}{|\mathbf{w}^H(\mathbf{I}_L\otimes\mathbf{A}_c)\mathbf{s}|^2+\|\mathbf{w}^H(\mathbf{I}_L\otimes\mathbf{A}_b\mathbf{G})\|^2+\sigma_{n,R}^2\|\mathbf{w}\|_2^2}\\ s.t.\quad &\frac{|\mathbf{h}_{m_r,C}\mathbf{g}_{m_r}|^2}{\sum_{i\neq m_r}|\mathbf{h}_{m_r,C}\mathbf{g}_i|^2+\frac{1}{L}\|(\mathbf{I}_L\otimes\mathbf{h}_{m_r,R})\mathbf{s}\|_2^2+\sigma_{n,C}^2}\ge t,\\ &m_r=1,\ldots,M_r,\\ &\|\mathbf{G}\|_F^2\le P_c,\end{aligned}\tag{15}$$

which can be recast as

$$\begin{aligned}\min_{\mathbf{G}} \quad & \|\mathbf{w}^H(\mathbf{I}_L \otimes \mathbf{A}_b\mathbf{G})\|^2 \\ s.t. \quad & \frac{|\mathbf{h}_{m_r,C}\mathbf{g}_{m_r}|^2}{\sum_{i\neq m_r}|\mathbf{h}_{m_r,C}\mathbf{g}_i|^2+\frac{1}{L}\|(\mathbf{I}_L \otimes \mathbf{h}_{m_r,R})\mathbf{s}\|_2^2+\sigma_{n,C}^2} \geq t, \\ & m_r = 1,\ldots,M_r, \\ & \|\mathbf{G}\|_F^2 \leq P_c. \end{aligned} \tag{16}$$

The objective function of the problem (Equation 16) can be rewritten as

$$\begin{aligned}\|\mathbf{w}^H(\mathbf{I}_L \otimes \mathbf{A}_b\mathbf{G})\|^2 &= \mathbf{w}^H(\mathbf{I}_L \otimes \mathbf{A}_b\mathbf{G}\mathbf{G}^H\mathbf{A}_b^H)\mathbf{w} \\ &= \sum_{l=1}^{L}\mathbf{w}_l^H\mathbf{A}_b\mathbf{G}\mathbf{G}^H\mathbf{A}_b^H\mathbf{w}_l \\ &= \mathbf{g}^H(\mathbf{I}_{M_r} \otimes \boldsymbol{\Upsilon})\mathbf{g}, \end{aligned} \tag{17}$$

where $\mathbf{g} = \left[\mathbf{g}_1^T,\ldots,\mathbf{g}_{M_r}^T\right]^T$, $\boldsymbol{\Upsilon} = \mathbf{A}_b^H\left(\sum_{l=1}^{L}\mathbf{w}_l\mathbf{w}_l^H\right)$ and $\mathbf{A}_b \succeq \mathbf{0}$ is the semidefinite matrix,.

According to Equation (17), Equation (16) is rewritten as follows

$$\begin{aligned}\min_{\mathbf{g}} \quad & \mathbf{g}^H(\mathbf{I}_{M_r} \otimes \boldsymbol{\Upsilon})\mathbf{g} \\ s.t. \quad & t\sum_{i\neq m_r}|\mathbf{h}_{m_r,C}\mathbf{g}_i|^2 - |\mathbf{h}_{m_r,C}\mathbf{g}_{m_r}|^2 \leq -t\left(C_s+\sigma_{n,C}^2\right) \\ & m_r = 1,\ldots,M_r, \\ & \|\mathbf{g}\|_2^2 \leq P_c, \end{aligned} \tag{18}$$

where $C_s = \frac{1}{L}\|(\mathbf{I}_L \otimes \mathbf{h}_{m_r,R})\mathbf{s}\|_2^2$. Noted that the first constraint of the problem (Equation 18) is actually the difference of convex functions. Therefore, the difference of convex programing (DCP) [35] can be utilised to solve this problem. Before deploying the DCP, we introduce a lemma below.

Lemma 1 *For the function* $f(\mathbf{x}) = |\mathbf{h}^H\mathbf{x}|^2$, the following is satisfied

$$f(\mathbf{x}) \geq 2\Re\left(\mathbf{x}_n^H\mathbf{H}\mathbf{x}\right) - f(\mathbf{x}_n), \tag{19}$$

where $\mathbf{H} = \mathbf{h}\mathbf{h}^H$, $\mathbf{x}_n$ *denotes the current point and the equality holds if and only if* $\mathbf{x} = \mathbf{x}_n$.

Proof: Firstly, we define a real-value function

$$g(\mathbf{x}_r) = \mathbf{x}_r^T\mathbf{H}_r\mathbf{x}_r \tag{20}$$

where

$$\mathbf{x}_r = \begin{bmatrix}\Re\{\mathbf{x}\}\\ \Im\{\mathbf{x}\}\end{bmatrix}, \quad \mathbf{H}_r = \begin{bmatrix}\Re\{\mathbf{H}\} & -\Im\{\mathbf{H}\}\\ \Im\{\mathbf{H}\} & \Re\{\mathbf{H}\}\end{bmatrix}. \tag{21}$$

Meanwhile, it is observed that $f(\mathbf{x}) = g(\mathbf{x}_r)$ and $\mathbf{H}_r = \mathbf{H}_r^T$. Then, we have

$$\begin{aligned} g(\mathbf{x}_r) &\geq g(\mathbf{x}_{r,n}) + \nabla^T g(\mathbf{x}_{r,n})(\mathbf{x}_r - \mathbf{x}_{r,n}) \\ &= \mathbf{x}_{r,n}^T\mathbf{H}_r\mathbf{x}_{r,n} + \mathbf{x}_{r,n}^T(\mathbf{H}_r + \mathbf{H}_r^T)(\mathbf{x}_r - \mathbf{x}_{r,n}) \\ &= \mathbf{x}_{r,n}^T\mathbf{H}_r\mathbf{x}_{r,n} + 2\mathbf{x}_{r,n}^T\mathbf{H}_r(\mathbf{x}_r - \mathbf{x}_{r,n}) \\ &= 2\mathbf{x}_{r,n}^T\mathbf{H}_r\mathbf{x}_r - \mathbf{x}_{r,n}^T\mathbf{H}_r\mathbf{x}_{r,n} \\ &= 2\Re\left(\mathbf{x}_n^H\mathbf{H}\mathbf{x}\right) - g(\mathbf{x}_{r,n}) \\ &= 2\Re\left(\mathbf{x}_n^H\mathbf{H}\mathbf{x}\right) - f(\mathbf{x}_n), \end{aligned} \tag{22}$$

where $\mathbf{x}_{r,n}$ is similarly defined as Equation (21). According to Equations (20) and (22), we conclude that the inequality Equation (19) is always held, thereby completing the proof.

According to Lemma 1, we need to solve the following problem at each iteration of DCP

$$\begin{aligned}\min_{\mathbf{g}} \quad & \mathbf{g}^H(\mathbf{I}_{M_r} \otimes \boldsymbol{\Upsilon})\mathbf{g} \\ s.t. \quad & t\sum_{i\neq m_r}|\mathbf{h}_{m_r,C}\mathbf{g}_i|^2 - 2\Re\left(\mathbf{g}_{m_r,n}^H\mathbf{h}_{m_r,C}^H\mathbf{h}_{m_r,C}\mathbf{g}_{m_r}\right) \\ & \leq -t\left(C_s+\sigma_{n,C}^2\right) - \mathbf{g}_{m_r,n}^H\mathbf{h}_{m_r,C}^H\mathbf{h}_{m_r,C}\mathbf{g}_{m_r,n}, \\ & m_r = 1,\ldots,M_r, \\ & \|\mathbf{g}\|_2^2 \leq P_c, \end{aligned} \tag{23}$$

which is convex and can be solved by CVX [39]. Note that the first inequality constraint of Equation (18) will be automatically satisfied since the left-hand side of the first constraint of Equation (23) is the upper bound of the counterpart of Equation (18).

3.3 | Update the transmit signal s

For the fixed t, $\mathbf{w}$ and $\mathbf{G}$, the problem with respect to $\mathbf{s}$ is

$$\begin{aligned}\max_{\mathbf{s}} \quad & \frac{|\mathbf{w}^H(\mathbf{I}_L \otimes \mathbf{A}_t)\mathbf{s}|^2}{|\mathbf{w}^H(\mathbf{I}_L \otimes \mathbf{A}_c)\mathbf{s}|^2 + \|\mathbf{w}^H(\mathbf{I}_L \otimes \mathbf{A}_b\mathbf{G})\|^2 + \sigma_{n,R}^2\|\mathbf{w}\|_2^2} \\ s.t. \quad & \frac{|\mathbf{h}_{m_r,C}\mathbf{g}_{m_r}|^2}{\sum_{i\neq m_r}|\mathbf{h}_{m_r,C}\mathbf{g}_i|^2+\frac{1}{L}\|(\mathbf{I}_L \otimes \mathbf{h}_{m_r,R})\mathbf{s}\|_2^2+\sigma_{n,C}^2} \geq t, \\ & m_r = 1,\ldots,M_r, \\ & \|\mathbf{s}\|_2^2 = 1, \\ & \|\mathbf{s} - \mathbf{s}_0\|_2^2 \leq \xi. \end{aligned} \tag{24}$$

It can be rewritten as

$$\mathcal{P}_1\begin{cases}\max\limits_{\mathbf{s}} & \dfrac{|\mathbf{w}^H(\mathbf{I}_L\otimes\mathbf{A}_t)\mathbf{s}|^2}{\mathbf{s}^H\boldsymbol{\Xi}(\mathbf{w},\mathbf{G})\mathbf{s}}\\ s.t. & \mathbf{s}^H\mathbf{D}_{m_r}\mathbf{s}\le p_{m_r}, m_r=1,\ldots,M_r,\\ & \|\mathbf{s}\|_2^2=1,\\ & \|\mathbf{s}-\mathbf{s}_0\|_2^2\le\xi,\end{cases}\tag{25}$$

where

$$\begin{aligned}\mathbf{D}_{m_r}&=\left(\mathbf{I}_L\otimes\mathbf{h}_{m_r,R}^H\right)\left(\mathbf{I}_L\otimes\mathbf{h}_{m_r,R}\right),\\ p_{m_r}&=\frac{L}{t}|\mathbf{h}_{m_r,C}\mathbf{g}_{m_r}|^2-L\sum_{i\neq m_r}|\mathbf{h}_{m_r,C}\mathbf{g}_i|^2-L\sigma_{n,C}^2,\\ \boldsymbol{\Xi}(\mathbf{w},\mathbf{G})&=\left(\mathbf{I}_L\otimes\mathbf{A}_c^H\right)\mathbf{w}\mathbf{w}^H\left(\mathbf{I}_L\otimes\mathbf{A}_c\right)\\ &\quad+\sigma_{n,R}^2\|\mathbf{w}\|_2^2\mathbf{I}_{N_tL}+\|\mathbf{w}^H(\mathbf{I}_L\otimes\mathbf{A}_b\mathbf{G})\|^2\mathbf{I}_{N_tL}.\end{aligned}\tag{26}$$

Then, we can equivalently reformulate the problem (Equation 25) as [21, 40]

$$\mathcal{P}_2\begin{cases}\max\limits_{\mathbf{s}} & \dfrac{|\mathbf{w}^H(\mathbf{I}_L\otimes\mathbf{A}_t)\mathbf{s}|}{\sqrt{\mathbf{s}^H\boldsymbol{\Xi}(\mathbf{w},\mathbf{G})\mathbf{s}}}\\ s.t. & \mathbf{s}^H\mathbf{D}_{m_r}\mathbf{s}\le p_{m_r}, m_r=1,\ldots,M_r,\\ & \|\mathbf{s}\|_2^2\le 1, \Re\left(\mathbf{s}_0^H\mathbf{s}\right)\ge 1-\xi/2.\end{cases}\tag{27}$$

Noted that the two optimization problems $\mathcal{P}_1$ and $\mathcal{P}_2$ share the same optimal solution.

Lemma 2 *Problem $\mathcal{P}_2$ can be equivalently recast into*

$$\mathcal{P}_3\begin{cases}\max\limits_{\mathbf{s}} & \dfrac{\Re\left(\mathbf{w}^H(\mathbf{I}_L\otimes\mathbf{A}_t)\mathbf{s}\right)}{\sqrt{\mathbf{s}^H\boldsymbol{\Xi}(\mathbf{w},\mathbf{G})\mathbf{s}}}\\ s.t. & \mathbf{s}^H\mathbf{D}_{m_r}\mathbf{s}\le p_{m_r}, m_r=1,\ldots,M_r,\\ & \|\mathbf{s}\|_2^2\le 1,\ \Re\left(\mathbf{s}_0^H\mathbf{s}\right)\ge 1-\xi/2,\\ & \Re\left(\mathbf{w}^H(\mathbf{I}_L\otimes\mathbf{A}_t)\mathbf{s}\right)\ge 0.\end{cases}\tag{28}$$

Proof: According to problem (Equation 12), it is seen that

$$\tilde{\mathbf{w}}=\mathbf{w}e^{j\psi},\tag{29}$$

is still the optimal solution of Equation (12), where $\mathbf{w}$ is obtained from Equation (13) and $\psi=[0,2\pi]$ denotes the phase-shift. Hence, substituting $\mathbf{w}$ by $\tilde{\mathbf{w}}$ does not change the solution of the problem $\mathcal{P}_2$. Let us denote the optimal solution of $\mathcal{P}_2$ as $\mathbf{s}^\star$ and suppose $\psi=\arg(\mathbf{w}^H(\mathbf{I}_L\otimes\mathbf{A}_t)\mathbf{s}^\star)$. To simplify notations, we rewrite

$$\mathbf{w}^H(\mathbf{I}_L\otimes\mathbf{A}_t)\mathbf{s}^\star=r(\cos\psi+j\sin\psi),\tag{30}$$

where $r\ge 0$ denotes the modulus of $\mathbf{w}^H(\mathbf{I}_L\otimes\mathbf{A}_t)\mathbf{s}^\star$. Then, it is derived that

$$\begin{aligned}\Re\left(\tilde{\mathbf{w}}^H(\mathbf{I}_L\otimes\mathbf{A}_t)\mathbf{s}^\star\right)&=\Re\left(e^{-j\psi}\mathbf{w}^H(\mathbf{I}_L\otimes\mathbf{A}_t)\mathbf{s}^\star\right)\\&=\Re\left(re^{-j\psi}(\cos\psi+j\sin\psi)\right)\\&=\Re\left(re^{-j\psi}e^{j\psi}\right)\\&=|\tilde{\mathbf{w}}^H(\mathbf{I}_L\otimes\mathbf{A}_t)\mathbf{s}^\star|.\end{aligned}\tag{31}$$

According to Equation (31) and $r\ge 0$, the last constraint of $\mathcal{P}_3$ is automatically satisfied for the point $\mathbf{s}^\star$. Hence, we conclude that $\mathbf{s}^\star$ is also feasible for Equation (28) and the objective value $v(\mathcal{P}_3)\ge v(\mathcal{P}_2)$. Moreover, it is noted that any feasible point $\mathbf{s}$ for $\mathcal{P}_3$ is also feasible to $\mathcal{P}_2$. Meanwhile, it has $v(\mathcal{P}_3)\le v(\mathcal{P}_2)$ at the same point [35]. Consequently, we can conclude that $v(\mathcal{P}_3)=v(\mathcal{P}_2)$, and any optimal solution of $\mathcal{P}_3$ is also optimal to $\mathcal{P}_2$, thereby completing the proof.

Notice that the objective function of the problem $\mathcal{P}_3$ consists of the ratio between a nonnegative concave function and a positive convex function. Thus, by employing the Dinkelbach-based algorithm, problem $\mathcal{P}_3$ can be solved via solving a series of convex problems. At each iteration of the Dinkelbach-based algorithm, the problem to be solved takes the form

$$\begin{aligned}\max_{\mathbf{s}}\quad & \Re\left(\mathbf{w}^H(\mathbf{I}_L\otimes\mathbf{A}_t)\mathbf{s}\right)-\mu\sqrt{\mathbf{s}^H\boldsymbol{\Xi}(\mathbf{w},\mathbf{G})\mathbf{s}}\\ s.t.\quad & \mathbf{s}^H\mathbf{D}_{m_r}\mathbf{s}\le p_{m_r}, m_r=1,\ldots,M_r,\\ & \|\mathbf{s}\|_2^2\le 1,\ \Re\left(\mathbf{s}_0^H\mathbf{s}\right)\ge 1-\xi/2,\\ & \Re\left(\mathbf{w}^H(\mathbf{I}_L\otimes\mathbf{A}_t)\mathbf{s}\right)\ge 0,\end{aligned}\tag{32}$$

where μ is updated iteratively.

The Dinkelbach-based algorithm for solving the problem $\mathcal{P}_3$ is summarised in Algorithm 1.

Algorithm 1 Dinkelbach-based Solver for $\mathcal{P}_3$

Input: $\mathbf{w}$, $\mathbf{s}_0$, ζ_1, $\mathbf{A}_t$, $\mathbf{G}$, p_{m_r} and $\mathbf{D}_{m_r}, m_r=1,\ldots,M_r$

1: Set $r=0$, $\mu_r=0$

2: **repeat**

3: Find the optimal solution $\mathbf{s}_r$ of Equation (32) by CVX

4: Calculate the value: $F(\mu_r)=\Re(\mathbf{w}^H(\mathbf{I}_L\otimes\mathbf{A}_t)\mathbf{s}_r)-\mu_r\sqrt{\mathbf{s}_r^H\boldsymbol{\Xi}(\mathbf{w},\mathbf{G})\mathbf{s}_r}$.

5: Update $\mu_r=\Re(\mathbf{w}^H(\mathbf{I}_L\otimes\mathbf{A}_t)\mathbf{s}_r)/\sqrt{\mathbf{s}_r^H\boldsymbol{\Xi}(\mathbf{w},\mathbf{G})\mathbf{s}_r}$

6: Set $r\leftarrow r+1$

7: **until** $F(\mu_r)\le\zeta_1$ or maximum iteration time reached

Output: $\mathbf{s}^\star=\mathbf{s}_r$.

Algorithm 2 Alternating Maximisation Algorithm for Problem (Equation 10)

Input: $\sigma_{n,R}^2$, $\sigma_{n,C}^2$, θ_t, θ_c, ξ, ζ_2, $\mathbf{A}_t$, $\mathbf{A}_c$, $\mathbf{A}_b$, $\mathbf{H}_R$ and $\mathbf{H}_C$

1: Set $n = 0$ and initial variables $\{t^{(0)}, \mathbf{w}^{(0)}, \mathbf{s}^{(0)}, \mathbf{G}^{(0)}\}$
2: **repeat**
3: Update $\mathbf{w}^{(n+1)}$ as Equation (13)
4: Update $\mathbf{G}^{(n+1)}$ via solving Equation (23)
5: Update $\mathbf{s}^{(n+1)}$ through Algorithm 1
6: Update $\mathbf{t}^{(n+1)}$ as Equation (34)
7: Set $n \leftarrow n + 1$
8: **until**
$\left|\mathrm{SINR}_r^{(n)} + t^{(n)} - \mathrm{SINR}_r^{(n-1)} - t^{(n-1)}\right| \le \zeta_2$ or maximum iteration time reached

Output: $t^\star = t^{(n)}$, $\mathbf{w}^\star = \mathbf{w}^{(n)}$, $\mathbf{s}^\star = \mathbf{s}^{(n)}$, $\mathbf{G}^\star = \mathbf{G}^{(n)}$.

3.4 | Update the auxiliary variable t

For the given $\mathbf{s}$ and $\mathbf{G}$, the optimization problem corresponding with t is given by

$$\begin{aligned} \max_{t} \quad & t \\ s.t. \quad & \mathrm{SINR}_c^{m_r} \ge t, m_r = 1, \ldots, M_r. \end{aligned} \tag{33}$$

Hence, we can update it as follows

$$t = \max\left\{t_n, \arg\min_{m_r} \mathrm{SINR}_c^{m_r}\right\}, \tag{34}$$

where t_n denotes the value of t at the last iteration. Note that Equation (34) guarantees that t is monotonically non-decreasing with the iterations.

Based on the above discussion, the proposed AM algorithm for problem (Equation 10) is summarised in Algorithm 2.

3.5 | Computational complexity

It is observed that the overall computational burden of Algorithm 2 is linear with the number of outer iterations. Meanwhile, at each outer iteration, the closed-form solution of the radar receiver filter $\mathbf{w}$ is given by Equation (13) with the complexity of $\mathcal{O}(L^3N_r^3)$. Then, the precoding matrix $\mathbf{G}$ can be obtained by CVX in $\mathcal{O}(M_t^3M_r^3)$. As for the update of the radar waveform $\mathbf{s}$, the computational cost of Algorithm 1 is linear with the number of inner iterations I. At each inner iteration, the Dinkelbach-based method requires to solve problem (Equation 32) by CVX with the complexity of $\mathcal{O}(L^3N_t^3)$. In order to update the auxiliary variable t, the communication SINR for all users should be computed with the complexity of $\mathcal{O}(M_r(M_t^2 + L^2N_t^2))$. Finally, we can conclude that the total complexity of the proposed algorithm is $\mathcal{O}(L^3N_r^3 + M_t^3M_r^3 + I(L^3N_t^3) + M_r(M_t^2 + L^2N_t^2))$ at each outer iteration.

4 | SIMULATION RESULTS

In this section, numerical results are provided to evaluate the performance of the proposed method. Throughout the simulations, the antenna arrays are configured as uniform linear array (ULA) with half-wavelength inter-element spacing. We assume the colocated MIMO radar system equips with $N_t = 5$ transmit and $N_r = 5$ receiver antennas, respectively. Meanwhile, the MU-MISO communication system consists with $M_t = 6$ transmit antennas at the BS serving for $M_r = 2$ single-antenna users. The code length is set as $L = 16$. We utilise the Linear Frequency Modulation (LFM) as the radar reference waveform $\mathbf{s}_0$, while the space-time waveform matrix is given by [21]

$$\mathbf{S}_0(n_t, l) = \frac{e^{j2\pi n_t(l-1)/N_t} e^{j\pi(l-1)^2/N_t}}{\sqrt{LN_t}}, \tag{35}$$

where $\mathbf{s}_0 = \mathrm{vec}(\mathbf{S}_0)$. Without loss of generality, the total communication energy is set as $P_c = 1$ which is equal to the radar transmit energy. Consider a single target is located at $\theta_0 = 5°$ with the Doppler frequency $v_t = 0$ and $K = 2$ clutters are located at $\theta_1 = -20°$ and $\theta_2 = 28°$, respectively. The reflection parameter of the target is $\alpha_0 = 1$ and the corresponding parameter of the clutters are $\alpha_1 = 0.9$ and $\alpha_2 = 0.9$, respectively. For simplicity, the elements of the channel matrix $\mathbf{A}_b$, $\mathbf{H}_R$ and $\mathbf{H}_C$ are distributed as $\mathcal{CN}(0, 1)$. The initializations $\mathbf{w}^{(0)}$, $\mathbf{s}^{(0)}$ and $\mathbf{G}^{(0)}$ are randomly generated, whose entries are also distributed as $\mathcal{CN}(0, 1)$ and $t^{(0)} = 10^{-3}$. Lastly, we consider the termination criterion is $\zeta_1 = 10^{-1}$ (or reach the maximum iterations 30) for Algorithm 1, and $\zeta_2 = 10^{-6}$ (or reach the maximum iterations 50) for Algorithm 2.

4.1 | Performance comparison with different similarity levels

In this example, the radar and communication noise variance are assumed as $\sigma_{n,R}^2 = -15$ dB and $\sigma_{n,C}^2 = -15$ dB, respectively. We can first evaluate the convergence performance of the proposed AM Algorithm 2. Figure 2 compares the value of the objective function in Equation (11) versus the number of outer iterations with different values of the radar similarity parameter ξ. It is seen that the proposed method tends to always converge within around 25 iterations. Meanwhile, the larger optimal values are obtained as increasing the parameter ξ yields larger feasible sets. Note that the faster convergence can be achieved with the larger ξ, but, at the cost of poorer similarity to the chosen waveform.

Figure 3 shows the radar output SINR versus number of iterations. Similarly, the improved radar SINR can be achieved with the larger ξ. In Figure 4, we observe that the minimal

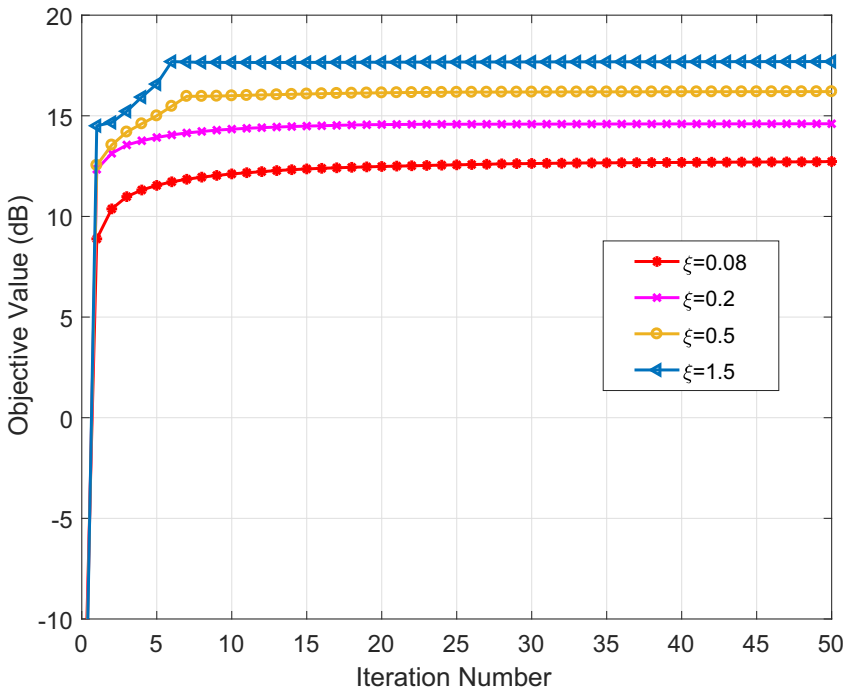

FIGURE 2 Objective value versus number of iterations

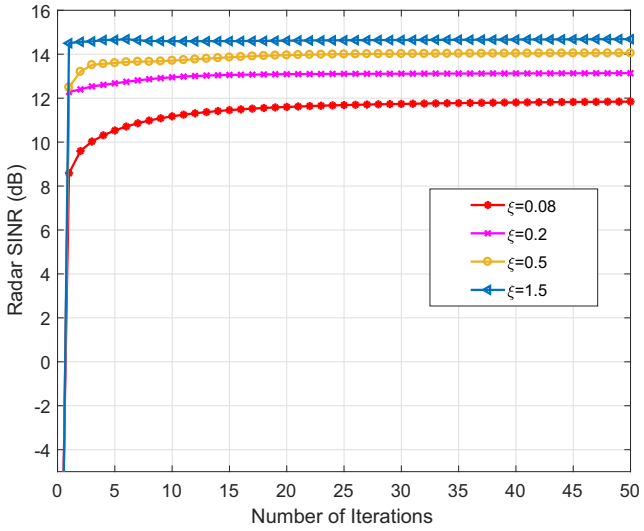

FIGURE 3 Radar output SINR versus number of iterations

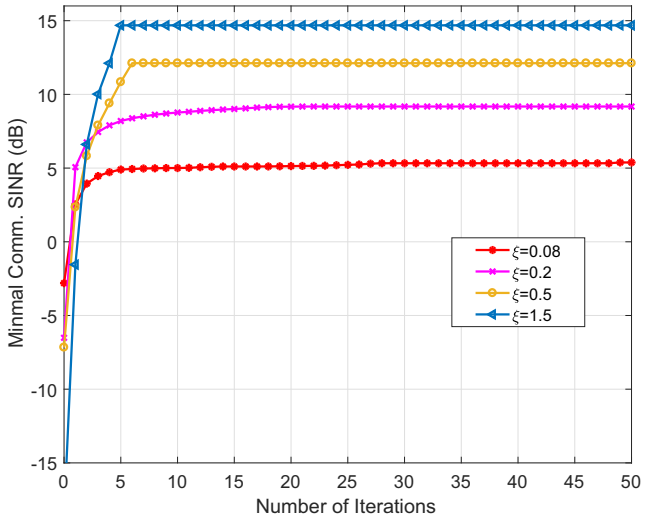

FIGURE 4 Minimal communication SINR versus number of iterations

SINR of users is monotonically increasing with iterations, which is consistent with our analysis for updating t in Equation (34). Based on the above, it is seen that the proposed method shows the favourable convergence in terms of the objective value, the radar SINR and the minimal SINR of users guarantee the performance of sensing and communication, respectively.

Figure 5 demonstrates the receiver beampatterns for the radar system. We observe that the single mainlobe is precisely aligned to the target while the nulls occur in the clutter directions. Figure 6 shows the ambiguity function for the designed waveform with different similarity levels. It is seen that the smaller ξ leads to the sharper peak, which is corresponding with the better resolution of range-Doppler. However, as illustrated in Figures 3 and 4, the smaller ξ corresponds to a lower radar and communication SINR. Thus, there is a trade-off between the SINR and the ambiguity property. For this purpose, we choose $\xi = 0.2$ in the sequel.

4.2 | Performance comparison with benchmark

In this example, we compare the proposed method with some benchmarks. In Figure 7, we compare the convergence performance of the proposed method with optimal t and the

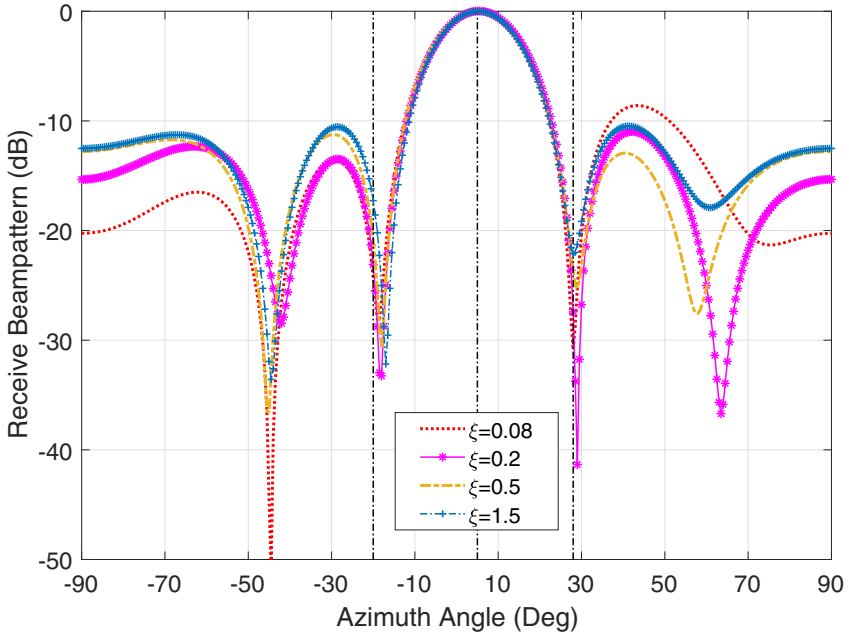

FIGURE 5 Receiver beampattern of the proposed method

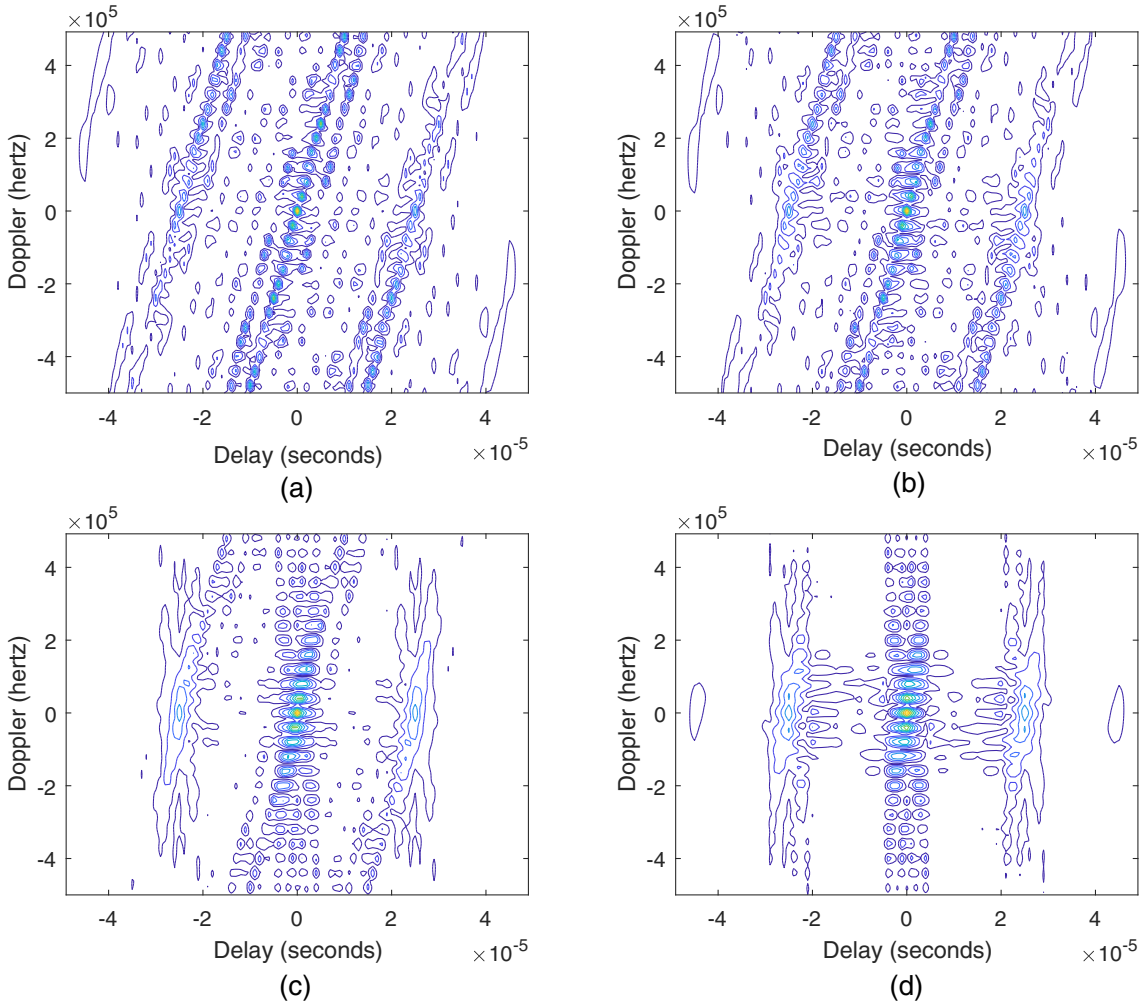

FIGURE 6 Ambiguity functions under different similarity level. (a) $\xi = 0.08$; (b) $\xi = 0.2$; (c) $\xi = 0.5$; (d) $\xi = 1.5$

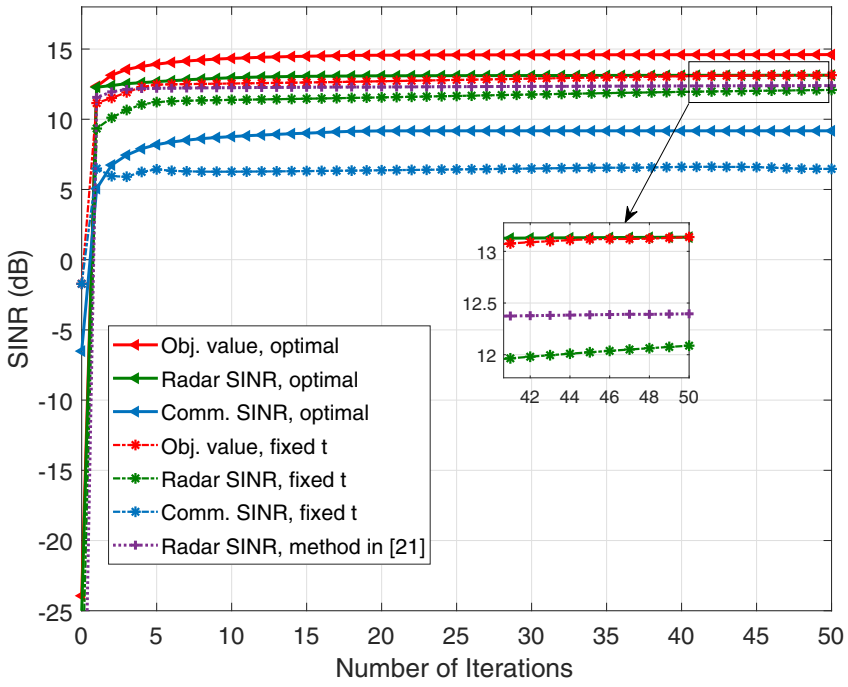

FIGURE 7 Convergence comparison for optimal t and fixed t

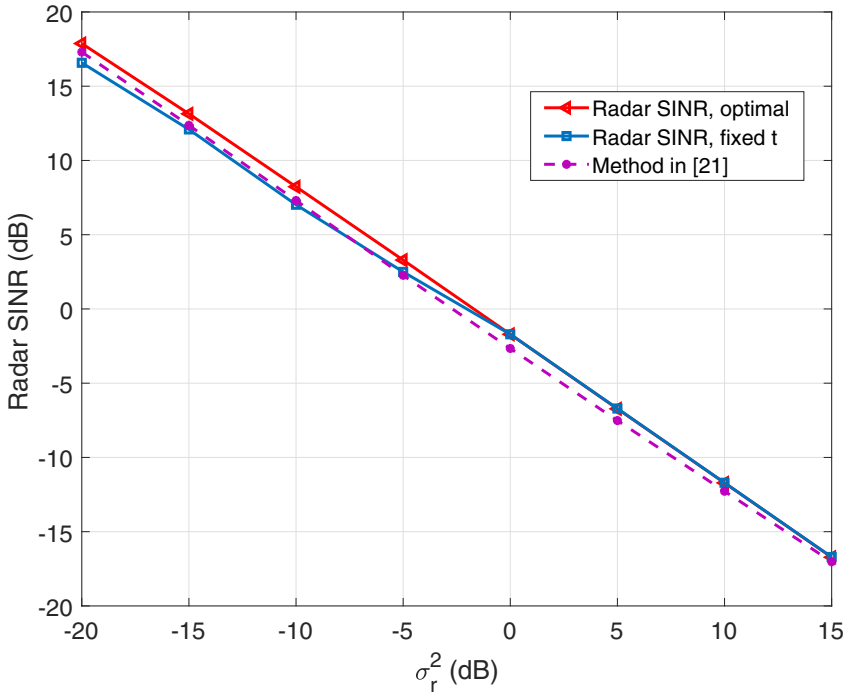

FIGURE 8 Achievable radar SINR with different σ_r^2

proposed method with fixed t. The noise power for radar and communication are set as $\sigma_{n,R}^2 = -15$ dB and $\sigma_{n,C}^2 = -15$ dB, respectively. It is seen that the proposed method with optimal t has better overall performance compared to the proposed method with fixed t and method in Ref. [21] which consider maximising the radar SINR and guaranteeing the capacity of communication.

Figure 8 shows the achievable radar SINR with the different radar noise power. The communication noise power is fixed as $\sigma_{n,C}^2 = -15$ dB. If the radar noise power σ_r^2 is lower than 0 dB, the proposed method with optimal t obtains higher radar SINR. Otherwise, the achievable SINR for these two methods are same. Meanwhile, the proposed method also has around 0.6 dB enhancement compared with the method due to the flexibility of performance trade-off. Figure 9 demonstrates the minimal achievable communication SINR with the different communication noise power. As expected, the proposed method with optimal t achieves the higher SINR

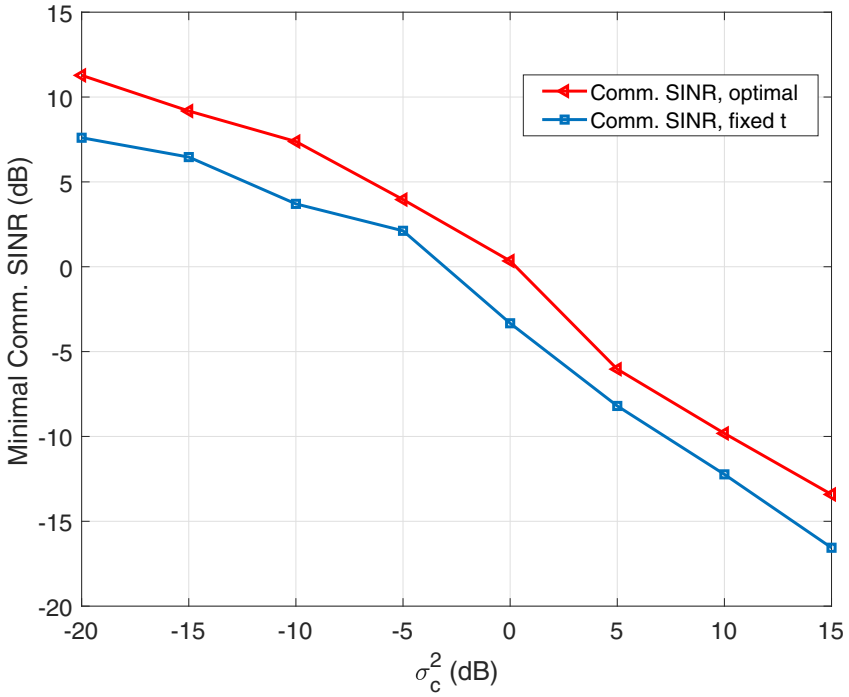

FIGURE 9 Achievable minimum communication SINR with different σ_c^2

compared with fixed t which shows the superiority of updating t in Algorithm 2. Combining Figures 8 and 9, it is concluded that the proposed method with the optimal t is able to achieve the better performance for both sensing and communication compared with the benchmark.

5 | CONCLUSION

We study the coexistence of MIMO radar and MU-MISO communication. By jointly designing the transmit waveform, the receiver filter bank and the precoding matrix, both the SINR for radar and the minimal SINR for communication users are maximised. However, the resulting problem is highly nonconvex and the optimization variables are coupled with each other. To overcome this, an AM-based algorithm is developed via combining the DCP and the Dinkelbach method. Compared with other design schemes, the proposed method does not need give any threshold for radar or communication metric. The simulation results show that the proposed method can achieve satisfactory performance both in radar and communication.

ACKNOWLEDGMENTS

This work was supported by the Luxembourg National Research Fund (FNR) through the SPRINGER Project, ref 12734677.

CONFLICT OF INTEREST

We declare that we have no financial and personal relationships with other people or organisations that can inappropriately influence our work, there is no professional or other personal interest of any nature or kind in any product, service and/or company that could be construed as influencing the position presented in, or the review of the manuscript.

DATA AVAILABILITY STATEMENT

The data that support the findings of this study are available in the supplementary material of this article.

ORCID

Tong Wei https://orcid.org/0000-0002-2104-2694

REFERENCES

1. Lin, X., Andrews, J.G., Ghosh, A.: Spectrum sharing for device-to-device communication in cellular networks. IEEE Trans. Wireless Commun. 13(12), 6727–6740 (2014)
2. Liu, F., et al.: Joint radar and communication design: applications, state-of-the-art, and the road ahead. IEEE Trans. Commun. 68(6), 3834–3862 (2020)
3. Chen, H., et al.: Tensor decompositions in wireless communications and MIMO radar. IEEE Journal of Selected Topics in Signal Processing. 15(3), 438–453 (2021)
4. Li, B., Petropulu, A.P.: Joint transmit designs for coexistence of MIMO wireless communications and sparse sensing radars in clutter. IEEE Trans. Aero. Electron. Syst. 53(6), 2846–2864 (2017)
5. Li, B., Petropulu, A.P., Trappe, W.: Optimum co-design for dpectrum sharing between matrix completion based MIMO radars and a MIMO communication system. IEEE Trans. Signal Process. 64(17), 4562–4575 (2016)
6. Mishra, K.V., et al.: Toward millimeter-wave joint radar communications: a signal processing perspective. IEEE Signal Process. Mag. 36(5), 100–114 (2019)
7. Cheng, Z., et al.: Communication-aware waveform design for MIMO radar with good transmit beampattern. IEEE Trans. Signal Process. 66(21), 5549–5562 (2018)
8. Alaee-Kerharoodi, M., et al.: Information theoretic approach for waveform design in coexisting MIMO radar and MIMO communications.

2020 IEEE International Conference on Acoustics, Speech and Signal Processing, Barcelona, Spain, pp. 1–5 (2020)
9. Raei, E., Alaee-Kerahroodi, M., Bhavani Shankar, M.R.: Beampattern shaping for coexistence of cognitive MIMO radar and MIMO communications. 2020 IEEE 11th Sensor Array and Multichannel Signal Processing Workshop, Hangzhou, China, pp. 1–5 (2020)
10. Wu, L., et al.: Resource allocation in heterogeneously-distributed joint radar-communications under asynchronous bayesian tracking framework. arXiv (2021)
11. Liu, F., et al.: Toward dual-functional radar-communication systems: optimal waveform design. IEEE Trans. Signal Process. 66(16), 4264–4279 (2018)
12. Hassanien, A., et al.: Phase-modulation based dual-function radar-communications. IET Radar Sonar Navig. 10(8), 1411–1421 (2016)
13. Wang, X., Hassanien, A., Amin, M.G.: Dual-function MIMO radar communications system design via sparse array optimization. IEEE Trans. Aero. Electron. Syst. 55(3), 1213–1226 (2019)
14. Cheng, Z., et al.: Transmit sequence design for dual-function radar-communication system with one-bit DACs. IEEE Trans. Wireless Commun. 20(9), 5846–5860 (2021)
15. Cheng, Z., et al.: Hybrid beamforming for wideband OFDM dual function radar communications. 2021 IEEE International Conference on Acoustics, Speech and Signal Processing, Toronto, ON, Canada, pp. 8238–8242 (2021)
16. Ahmed, A., Zhang, Y.D., Himed, B.: Distributed dual-function radar-communication MIMO system with optimized resource allocation. 2019 IEEE Radar Conference, Boston, MA, USA, pp. 1–5 (2019)
17. Dokhanchi, S.H., et al.: A mmWave automotive joint radar-communications system. IEEE Trans. Aero. Electron. Syst. 55(3), 1241–1260 (2019)
18. Dokhanchi, S.H., et al.: Adaptive waveform design for automotive joint radar-communication systems. IEEE Trans. Veh. Technol. 70(5), 4273–4290 (2021)
19. Xu, C., Clerckx, B., Zhang, J.: Multi-antenna joint radar and communications: precoder optimization and weighted sum-rate vs probing power tradeoff. IEEE Access. 8, 173974–173982 (2020)
20. He, X., Huang, L.: Joint MIMO communication and MIMO radar under different practical waveform constraints. IEEE Trans. Veh. Technol. 69(12), 16342–16347 (2020)
21. Qian, J., et al.: Joint system design for coexistence of MIMO radar and MIMO communication. IEEE Trans. Signal Process. 66(13), 3504–3519 (2018)
22. Qian, J., et al.: Joint optimization of the spectral coexistence of radar and communications system. 2020 IEEE Radar Conference, Florence, Italy, pp. 1–5 (2020)
23. Alaee-Kerahroodi, M., et al.: Discrete-phase sequence design for coexistence of MIMO radar and MIMO communications. 2019 IEEE 20th International Workshop on Signal Processing Advances in Wireless Communications, Cannes, France, pp. 1–5 (2019)
24. Liu, X., et al.: Joint transmit beamforming for multiuser MIMO communications and MIMO radar. IEEE Trans. Signal Process. 68, 3929–3944 (2020)
25. Qian, J., et al.: Transmit designs for spectral coexistence of MIMO radar and MIMO communication systems. IEEE Trans. Cir. Sys. 65(2), 2072–2076 (2018)
26. Bao, D., et al.: A precoding OFDM MIMO radar coexisting with a communication system. IEEE Trans. Aero. Electron. Syst. 55(4), 1864–1877 (2019)
27. Grossi, E., Lops, M., Venturino, L.: Energy efficiency optimization in radar-communication spectrum sharing. IEEE Trans. Signal Process. 69, 3541–3554 (2021)
28. He, Q., et al.: Performance gains from cooperative MIMO radar and MIMO communication systems. IEEE Signal Process. Lett. 26(1), 194–198 (2019)
29. Shi, C., et al.: Power minimization-based robust OFDM radar waveform design for radar and communication systems in coexistence. IEEE Trans. Signal Process. 66(5), 1316–1330 (2018)
30. Liu, Y., et al.: Super-resolution range and velocity estimations with OFDM integrated radar and communications waveform. IEEE Trans. Veh. Technol. 69(10), 11659–11672 (2020)
31. Shi, C., et al.: Joint optimization scheme for subcarrier selection and power allocation in multicarrier dual-function radar-communication system. IEEE Syst. J. 15(1), 947–958 (2021)
32. Chiriyath, A.R., Paul, B., Bliss, D.W.: Simultaneous radar detection and communications performance with clutter mitigation. 2017 IEEE Radar Conference (RadarConf), Seattle, WA, USA, pp. 0279–0284 (2017)
33. Liu, Y., et al.: Joint range and angle estimation for an integrated system combining MIMO radar with OFDM communication. Multidimens. Syst. Signal Process. 30(2), 661–687 (2019)
34. Jara-Moroni, F., Pang, J.-S., Wachter, A.: A study of the difference-of-convex approach for solving linear programs with complementarity constraints. Math. Program. 169(1), 221–254 (2018)
35. Dinkelbach, W.: On nonlinear fractional programming. Manag. Sci. 13(7), 492–498 (1967)
36. Liu, Y., Dai, Y., Luo, Z.: Max-Min fairness linear transceiver design for a multiuser MIMO interference channel. IEEE Trans. Signal Process. 61(9), 2413–2423 (2013)
37. Wu, L., Palomar, D.P.: Sequence design for spectral shaping via minimization of regularized spectral level ratio. IEEE Trans. Signal Process. 67(18), 4683–4695 (2019)
38. Wu, L., Babu, P., Palomar, D.P.: Transmit waveform/receive filter design for MIMO radar with multiple waveform constraints. IEEE Trans. Signal Process. 66(6), 1526–1540 (2018)
39. Grant, M., Boyd, S.: CVX: Matlab software for disciplined convex programming. Version 2.1, Feb 2016. [Online] Available: http://cvxr.com/cvx
40. Aubry, A., De Maio, A., Naghsh, M.M.: Optimizing radar waveform and Doppler filter bank via generalized fractional programming. IEEE Trans. Signal Process. 9(8), 1387–1399 (2015)

How to cite this article: Wei, T., Wu, L., Shankar Mysore Rama Rao, B.: Joint waveform and precoding design for coexistence of MIMO radar and MU-MISO communication. IET Signal Process. 16(7), 788–799 (2022). https://doi.org/10.1049/sil2.12110